ACCSCIENCE PUBLISHING

Eurasian Journal of Medicine and Oncology

ORIGINAL RESEARCH ARTICLE

Relationship between ischemic stroke and calcific aortic valve stenosis evaluated using Mendelian randomization and transcriptomic analysis

Rensheng Song[1†], Weihong Jin[1†], Huiling Zheng[1†], Sha He[2], Haoda Li[2], Junhui Zhong[2], Hongli Xian[1*], Yan Hu[3*], and Minghua Zhang[1*]

[1]Department of Cardiovascular Medicine, Key Laboratory of Biological Targeting Diagnosis, Therapy and Rehabilitation of Guangdong Higher Education Institutes, The Fifth Affiliated Hospital, Guangzhou Medical University, Guangzhou, Guangdong, China

[2]Key Laboratory of Biological Targeting Diagnosis, Therapy and Rehabilitation of Guangdong Higher Education Institutes, The Fifth Affiliated Hospital, Guangzhou Medical University, Guangzhou, Guangdong, China

[3]Department of Nursing, Key Laboratory of Biological Targeting Diagnosis, Therapy and Rehabilitation of Guangdong Higher Education Institutes, The Fifth Affiliated Hospital, Guangzhou Medical University, Guangzhou, Guangdong, China

[†]*These authors contributed equally to this work.*

***Corresponding authors:**
Hongli Xian
(649652448@qq.com);
Yan Hu
(Huyan86122319@126.com);
Minghua Zhang
(gzzhangminghua@163.com)

Citation: Song R, Jin W, Zheng H, *et al*. Relationship between ischemic stroke and calcific aortic valve stenosis evaluated using Mendelian randomization and transcriptomic analysis. *Eurasian J Med Oncol*. 2026;10(3):025360375.
doi: 10.36922/EJMO025360375

Received: September 03, 2025

Revised: December 30, 2025

Accepted: January 15, 2026

Published online: May 12, 2026

Abstract

Introduction: Aortic valve stenosis (AVS) is clinically associated with an increased risk of stroke and ischemic cerebrovascular events. However, previous studies on the relationship between aortic valve calcification and stroke have yielded inconsistent findings, and the causal link between ischemic stroke (IHS) and calcified AVS (CAVS) remains unclear due to confounding factors.

Objective: This study aimed to investigate the relationship between IHS and CAVS.

Methods: In the first part of the study, we explored the bidirectional causal relationship between IHS and CAVS using Mendelian randomization (MR). In the second part, we identified shared diagnostic biomarkers for the two diseases through differential gene expression analysis, weighted gene co-expression network analysis, and least absolute shrinkage and selection operator regression. Based on these biomarkers, an artificial neural network (ANN) diagnostic model was established to aid the diagnosis of both diseases.

Results: MR analysis suggested that genetically predicted IHS was associated with an increased risk of CAVS (p=0.0003, odds ratio [OR] = 1.2701, 95% confidence interval [CI]: 1.1153–1.4465), whereas CAVS did not exert a significant causal effect on IHS (p=0.2254, OR = 0.9751, 95% CI: 0.9361–1.0158). *FCGR2A*, *RBMS2*, *MAP1S*, *RCN3*, *HCK*, and *SLPI* were identified as shared diagnostic biomarkers for IHS and CAVS. Based on these six genes, an ANN diagnostic model was developed and demonstrated reliable diagnostic performance for both diseases.

Conclusion: Genetically predicted IHS appears to be associated with an increased risk of CAVS, while CAVS does not demonstrate a significant causal effect on IHS. *FCGR2A*, *RBMS2*, *MAP1S*, *RCN3*, *HCK*, and *SLPI* serve as shared diagnostic biomarkers for IHS and CAVS. The ANN-based diagnostic model incorporating these biomarkers showed strong predictive capability for both diseases.

Keywords: Ischemic stroke; Calcific aortic valve stenosis; Mendelian randomization; Biomarker; Diagnostic model

1. Introduction

The etiology of aortic valve stenosis (AVS) can be congenital, rheumatic, or calcific, with calcification being the most common cause.[1,2] Calcific AVS (CAVS) is characterized by progressive inflammation and gradual calcification of the aortic valve leaflets.[3] The prevalence of calcification increases with age, mainly affecting older adults, and occurs in 2–7% of individuals over 65 years of age.[4] Globally, CAVS has emerged as the third most prevalent cardiovascular disease among older adults, following coronary heart disease and hypertension.[5,6] Individuals with severe symptomatic CAVS face a 50% mortality risk within 2 years.[7] Despite advances in clinical knowledge and technology, the only effective treatment for severe CAVS remains surgery or transcatheter aortic valve replacement, which is not suitable for all patients.[8] To date, pharmacological interventions have not been shown to alter the course of CAVS. Therefore, there is an urgent need for studies to identify additional risk factors for CAVS, elucidate its pathophysiological mechanisms, and explore potential therapeutic targets to develop new therapeutic strategies aimed at slowing disease progression.

Cerebrovascular accidents, or strokes, are the second leading cause of death worldwide, accounting for approximately 5.5 million deaths annually.[9,10] Ischemic stroke (IHS), caused by interruption of cerebral blood flow, can lead to neurological impairment. IHS accounts for 70% of all stroke cases and is associated with an extremely high mortality rate.[11] Each year, over 9 million individuals are affected by IHS worldwide, imposing substantial burdens on healthcare systems.[12] The risk factors for IHS are diverse and include hypertension, diabetes, smoking habits, alcohol consumption, obesity, and inflammatory factors.[13] Recent studies indicate that early detection of IHS, followed by prompt intervention and specialized care at a dedicated stroke facility, can substantially lower the incidence of stroke-related complications and mortality.[11]

Stroke can occur in individuals with AVS. Reported stroke risk may increase after surgical treatment in patients with AVS.[14-16] A Danish retrospective cohort study found a significantly higher risk of IHS in patients with AVS compared with age- and sex-matched controls.[17] Autopsy studies have revealed that patients with aortic valve calcification (AVC) exhibit systemic embolization of calcium deposits in various arteries, including the brain, heart, kidneys, eyes, and peripheral circulation.[18] AVS is also associated with a high incidence of silent brain infarction,[19] which is linked to a two- to four-fold increased risk of future symptomatic stroke.[20] However, findings regarding the association between AVC and stroke have been inconsistent. Boon *et al.*[21] observed no significant increase in stroke incidence among patients with calcified aortic valves relative to those without calcification, while the Rotterdam Study[22] suggested that AVC is not correlated with a heightened risk of stroke. Observational and prospective clinical studies are often affected by various confounding factors or covariates, and the causal relationship between IHS and CAVS remains insufficiently investigated. Further research is therefore required to clarify the causal links between IHS and CAVS, as well as shared gene regulatory mechanisms, to inform the prevention and diagnosis of both conditions.

Bioinformatics offers an efficient and intuitive means for elucidating multifaceted molecular mechanisms underlying diseases and provides valuable information for fundamental medical research. Mendelian randomization (MR) is an innovative method increasingly used to investigate the causal relationships between modifiable factors and various diseases or traits.[23,24] This method overcomes key limitations of observational studies, particularly in establishing causality when randomized controlled trials are impractical, and helps mitigate confounding biases and the potential for reverse causation inherent in observational research.[23] As a component of artificial intelligence, machine learning has significantly expanded its applications in healthcare systems.[25] The integration of bioinformatics, MR analysis, and machine learning enhances the efficiency of various healthcare processes and provides a more sophisticated and reliable method for identifying potential biomarkers.[26] In this study, we first explored the bidirectional causal relationship between IHS and CAVS using MR. Next, we examined the possible connection between these two diseases at the transcriptomic level and assessed their interactions with immune cells through bioinformatics analysis.

2. Methods

2.1. Study design and ethical approval

Figure 1 illustrates the overall study design, including detailed procedures for selecting genetic variants and analytical methods.

This study used data from existing publicly available databases and did not involve any patient intervention or collection of new personal information; therefore, ethics committee approval was not required.

2.2. Data source

Summary statistics for IHS used in the MR analysis were obtained from the Integrative Epidemiology Unit Open Genome-Wide Association Study (GWAS) database (https://gwas.mrcieu.ac.uk/), which included 22,664 patients with IHS and 152,022 controls. GWAS

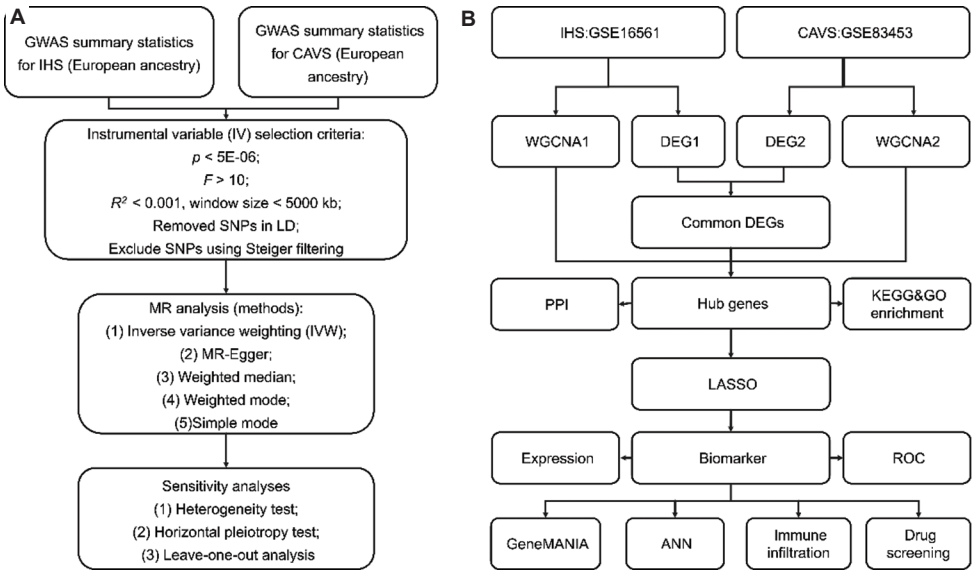

Figure 1. Study design and workflow. (A) MR analysis flowchart. (B) Transcriptome analysis flowchart.
Abbreviations: ANN: Artificial neural network; CAVS: Calcific aortic valve stenosis; DEG: Differentially expressed genes; GO: Gene Ontology; IHS: Ischemic stroke; KEGG: Kyoto Encyclopedia of Genes and Genomes; LASSO: Least absolute shrinkage and selection operator; LD: Linkage disequilibrium; MR: Mendelian randomization; PPI: Protein–protein interaction; ROC: Receiver operating characteristic; SNPs: Single-nucleotide polymorphisms; WGCNA: Weighted gene co-expression network analysis

summary statistics for CAVS used in the MR analysis were obtained from the FinnGen database,[27] which integrates genetic data on disease endpoints from the Finnish biobank and Finnish Health Registry (https://r10.finngen.fi/), comprising 9,870 patients with CAVS and 402,311 controls. All individuals in the original GWAS were of European ancestry.

Publicly available datasets for IHS and CAVS were retrieved from the Gene Expression Omnibus database. For IHS, GSE16561 (GPL6883) and GSE58294 (GPL570) were selected. GSE16561, used as the training set, included 39 patient blood samples with IHS and 24 healthy controls, while GSE58294, used as the validation set, comprised 23 controls and 69 cases. GSE83453 (GPL10558) and GSE12644 (GPL570) were selected for CAVS. GSE83453 served as the training set with 19 cases and eight controls, and GSE12644 as the validation set with 10 cases and 10 controls.

Detailed dataset information, including the number of patients and controls for both IHS and CAVS, is summarized in Table A1.

2.3. Selection of instrumental variables (IVs)

The validity of MR analysis hinges on three crucial prerequisites: first, the IVs must demonstrate a robust and significant correlation with the exposure variable; second, the IVs must be independent of any confounders of the relationship between the exposure and the observed outcome; and third, the association of IVs with outcomes should solely be mediated through the specific exposure being investigated.[28] For each exposure factor, IVs were selected according to the following steps:[29] (i) IVs were filtered using a significance threshold of $p<5\times10^{-6}$; (ii) linkage disequilibrium pruning was performed using the ieugwasr package's clump_data function (R^2 < 0.001 within a 5,000-kb window);[30] (iii) the exposure and outcome summary statistics were harmonized through the Harmonize function; (iv) IVs with *F*-statistics >10 were calculated and retained;[31] (v) single-nucleotide polymorphisms (SNPs) showing evidence of reverse causation or lacking statistical significance were excluded using Steiger filtering.[32,33]

2.4. MR analysis

Bidirectional two-sample MR analyses were performed using the TwoSampleMR (version 0.6.6)[34] and MR-PRESSO to assess the causal relationships between IHS and CAVS. Specifically, we performed forward MR analysis, treating IHS as the exposure and CAVS as the outcome, while reverse MR analysis considered CAVS as the exposure and IHS as the outcome. We used five evaluation methods for MR analysis: inverse variance weighted (IVW), MR-Egger, weighted median, simple mode, and weighted mode. Our MR findings relied primarily on the IVW algorithm, with other methods providing complementary validation.[35]

2.5. Sensitivity analysis

To evaluate the robustness of the MR results, a series of sensitivity analyses was performed, including assessments

of heterogeneity, horizontal pleiotropy, and leave-one-out analysis. Cochran Q test[36] was applied to assess heterogeneity, while horizontal pleiotropy was evaluated based on the intercept term of the MR-Egger regression model.[37] In addition, the MR-PRESSO[38] method was employed to identify and correct for outlier SNPs, which may indicate possible horizontal pleiotropic bias. Leave-one-out analysis was performed to assess whether any individual SNP disproportionately influenced the results.

2.6. Identification of differentially expressed genes (DEGs)

DEGs between the disease and control groups were identified using the Linear Models for Microarray Data (limma) package (version 3.50.1).[39] Differential expression analysis was conducted on the training datasets, and DEGs were identified in both the IHS and CAVS datasets using a significance threshold of $p<0.05$. To illustrate the expression levels of these DEGs, volcano plots and heatmaps were generated utilizing the ggplot2 package (version 3.3.2) and the heatmaps package (version 1.0.12).

2.7. Screening module genes using weighted gene co-expression network analysis (WGCNA)

To identify the genetic factors associated with both IHS and CAVS, disease grouping was used as a clinical trait in WGCNA to obtain a disease-related gene set. The R package WGCNA (version 1.70.3)[40] was used to perform WGCNA on all genes in the training datasets of both diseases to identify the key modules. Modules significantly correlated with disease traits were identified by evaluating module-trait and inter-module correlations. Key genes within these disease-associated modules were selected for further analysis.

2.8. Acquisition of key genes

Genes that were differentially expressed in both IHS and CAVS were recognized as potential crosstalk genes. Key genes were identified by intersecting these crosstalk genes with genes from the disease-associated modules obtained through WGCNA. These key genes may play critical roles in the shared pathogenic mechanisms linking IHS and CAVS.

2.9. Functional enrichment analysis of key genes

Gene Ontology (GO) and Kyoto Encyclopedia of Genes and Genomes (KEGG) pathway enrichment analyses were performed on key genes using the R language package clusterProfiler (version 4.2.2),[41] with a significance threshold of $p<0.05$. The findings were visualized using ggplot2.

2.10. Protein–protein interaction (PPI) networks of key genes

PPI analysis of key genes was performed using the STRING database (version 12.0).[42] Cytoscape software (version3.9.1)[43] was used to visualize the interaction network, with the confidence score set at 0.15.

2.11. Screening and identification of biomarkers

Based on the expression levels of key genes in IHS and CAVS, a machine learning algorithm, least absolute shrinkage and selection operator (LASSO) regression, was used to identify the candidate biomarkers. LASSO regression is a widely used data mining method for feature selection.[44] Using the glmnet R package (version 4.1.8),[45] LASSO regression was performed to select the first part of feature genes with the optimal tuning parameter determined through a 10-fold cross-validation based on the minimum criteria. Candidate biomarkers were identified by intersecting the LASSO-selected genes from the IHS and CAVS analyses.

The diagnostic performance of candidate biomarkers for each disease was assessed by receiver operating characteristic (ROC) curve analysis using the pROC R package. Genes with an area under the curve (AUC) >0.7 were considered potential biomarkers.

2.12. Expression of biomarkers

The expression patterns of the identified biomarkers were evaluated across IHS and CAVS datasets. The differences in biomarker expression between disease and control groups were assessed using the Wilcoxon rank-sum test. The results were visualized using violin plots generated with ggplot2.

2.13. Construction of artificial neural network (ANN) models

ANN models were constructed for both IHS and CAVS using the neuralnet R package (version 1.44.2). Biomarkers identified through the preceding analyses were used as model inputs. ANNs can derive classification rules from intricate data, enabling accurate categorization and the development of efficient and reliable diagnostic models.[46] In this study, the ANN architecture consisted of a single hidden layer containing three neurons. The number of neurons in the hidden layer was determined through a trial-and-error approach to balance the model complexity and predictive performance. Model accuracy was evaluated using ROC curve analysis for both training and validation datasets.

2.14. Construction of a co-expression network

A comprehensive co-expression network of the identified biomarkers was constructed using GeneMANIA[47]

(http://www.genemania.org/). This analysis aimed to elucidate the intricate interactions and shared biological pathways linking the biomarkers with other genes.

2.15. Immune infiltration analysis

Based on the gene signatures representing 28 immune cell types, single-sample gene set enrichment analysis (ssGSEA) was performed using the gene set variation analysis package[48] to estimate the abundance of immune cells in IHS and CAVS. Spearman's correlation analysis was used to investigate the intricate relationships between biomarker expression and immune cells, using a comprehensive gene expression matrix and detailed immune cell abundance data. The results were visualized using heatmaps. Additionally, the Wilcoxon rank-sum test was used to examine the disparities in immune cell infiltration levels across disease groups in the training datasets, with results displayed as box plots. These analyses may provide insights into the relationships among immune cells, biomarker genes, and diseases under investigation.

2.16. Screening of small-molecule drug candidates

Potential small-molecule drug candidates targeting the identified six biomarkers were screened using the DrugBank database (version 6.0).[49]

3. Results

3.1. Results of MR analysis and sensitivity analysis

IV screening identified 22 significant SNPs for forward MR analysis. Forward MR results indicated that genetically predicted IHS was associated with an increased risk of CAVS (IVW: p=0.0003, odds ratio [OR] = 1.2701, 95% confidence interval [CI]: 1.1153–1.4465) (Figure 2A-D). Sensitivity analyses revealed no evidence of heterogeneity or horizontal pleiotropy (p>0.05; Table 1). Leave-one-out sensitivity analysis demonstrated that exclusion of any individual SNP did not significantly affect the results, confirming the robustness and reliability of the findings (Figure 2E).

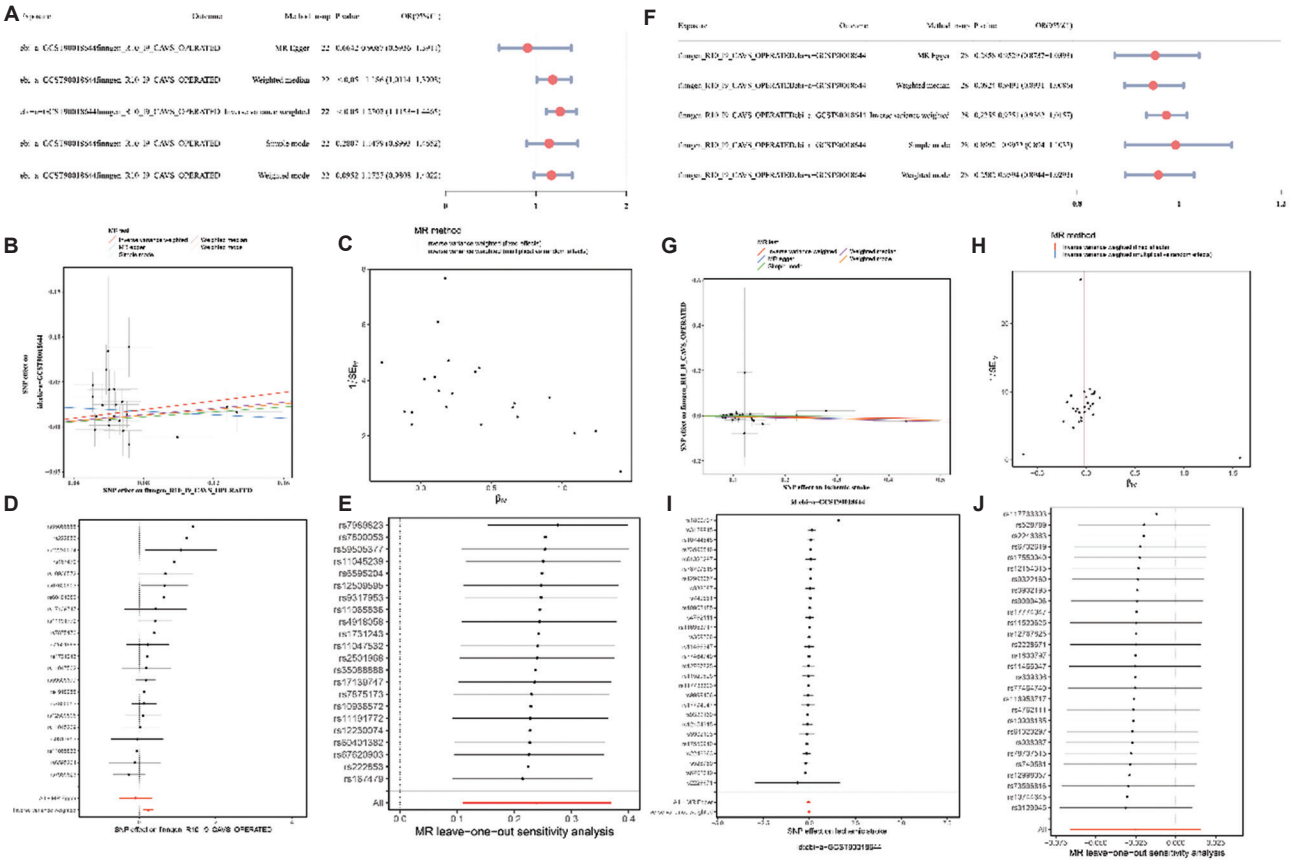

Figure 2. Results of Mendelian randomization (MR) analysis and sensitivity analyses. (A) Forest plot of odds ratio (OR) of forward MR results. (B) Scatter plot of forward MR analysis results. (C) Funnel plot of forward MR analysis results. (D) Forest plot of forward MR analysis results. (E) Forest plot of leave-one-out sensitivity analyses for forward MR results. (F) Forest plot of OR for reverse MR results. (G) Scatter plot of reverse MR analysis results. (H) Funnel plot of reverse MR analysis results. (I) Forest plot of reverse MR analysis results. (J) Forest plot of leave-one-out sensitivity analyses for reverse MR results.

Table 1. Sensitivity analysis of the association between IHS and CAVS

Exposure	Outcome	Method	Heterogeneity_Q	Q_df	Q_*p*-value	Egger_intercept	SE	*p*-value	MRPRESSO_*p*-value
IHS	CAVS	IVW	29.729	21	0.0975	0.0249	0.0155	0.1225	0.15
CAVS	IHS	IVW	15.1615	27	0.9671	0.0034	0.0058	0.5605	0.961

Abbreviations: CAVS: Calcific aortic valve stenosis; IHS: Ischemic stroke; IVW: Inverse variance weighted; SE: Standard error.

Additionally, IV screening identified 28 significant SNPs for reverse MR analysis. The results showed no significant causal effect of CAVS on IHS (IVW: p=0.2254, OR = 0.9751, 95% CI: 0.9361–1.0158) (Figure 2F-I). Consistent with these findings, sensitivity analyses indicated no heterogeneity or horizontal pleiotropy (p>0.05; Table 1). Leave-one-out sensitivity analysis further confirmed the robustness and reliability of the results, as exclusion of any single SNP did not significantly alter the estimates (Figure 2J).

3.2. Identification of DEGs

Comprehensive differential expression analysis identified 4,613 DEGs associated with IHS, including 2,322 upregulated and 2,291 downregulated genes, and 3,416 DEGs associated with CAVS, including 410 upregulated and 3,006 downregulated genes (Figure 3A and B). Volcano plots and heatmaps were generated to visualize the expression patterns of DEGs in both diseases. The top 10 upregulated and top 10 downregulated genes with the largest $\log_2$ fold-change were selected for further analysis (Figure 3C and D).

3.3. Screening of hub genes using WGCNA

To identify key genes for further analysis, we constructed a WGCNA network. For the IHS dataset, when the power parameter was set to 5, the resulting network structure closely mirrored a scale-free network distribution (Figure 3E). For the CAVS dataset, a scale-free network structure was achieved when the power parameter was adjusted to 8 (Figure 3F). Using the dynamic tree-cutting algorithm as the foundation, 10 gene modules were identified in IHS and seven gene modules in CAVS (Figure 3G and H). Module–trait correlation analysis revealed that the magenta and brown modules were most strongly associated with IHS grouping, whereas the blue and red modules showed the strongest correlations with CAVS grouping (Figure 3I and J). Accordingly, 2,312 IHS-related genes (WGCNA1) from the magenta and brown modules and 2,296 CAVS-related genes (WGCNA2) from the blue and red modules were selected for subsequent analyses.

3.4. Results of acquisition, functional enrichment analyses, and PPI network for key genes

Based on consistent expression trends across datasets, 893 DEGs were identified, including 424 upregulated and 469 downregulated genes (Figure 4A and B). Forty-one key genes were identified by intersecting common DEGs with genes derived from the WGCNA module (Figure 4C). Using these 41 key genes, a PPI network comprising 35 nodes and 40 edges was constructed using Cytoscape. Within the PPI network, the top five genes with the highest connectivity were hemopoietic cell kinase (*HCK*), chondroitin sulfate synthase 1, caspase 4, IQ motif containing GTPase activating protein 1, and recombinant forkhead box P1 (Figure 4D).

GO functional enrichment analysis of the 41 key genes identified 213 biological process terms, 22 cellular component terms, and 43 molecular function terms. The top five significantly enriched GO terms (p<0.05) are shown in Figure 4E. GO analysis indicated that these key genes were primarily localized to the membrane raft, membrane microdomain, the cell cortex, the lateral plasma membrane, and caveolae. They were mainly involved in biological processes such as ameboidal-type cell migration, regulation of epithelial cell migration, regulation of cellular component size, epithelial cell migration, and epithelial migration. Molecular function analysis revealed enrichment in small GTPase binding, GTPase binding, actin filament binding, DNA-binding transcriptional repressor activity, and RNA polymerase II-specific activity.

The KEGG pathway enrichment analysis showed that the 41 key genes were mainly enriched in the chemokine signaling pathway, Kaposi sarcoma-associated herpes virus infection, Fc gamma receptor-mediated phagocytosis, breast cancer, and glycosaminoglycan biosynthesis-chondroitin sulfate/dermatan sulfate (Figure 4F).

3.5. Screening and identification of biomarkers

LASSO regression analysis was performed on the 41 key genes. A total of 22 and eight representative diagnostic genes were identified for IHS and CAVS, respectively (Figure 5A-D). Intersection of LASSO-selected genes from both diseases yielded six candidate biomarkers: Fc gamma receptor IIa (*FCGR2A*), RNA-binding motif single-stranded-interacting protein 2 (*RBMS2*), microtubule-associated protein 1S (*MAP1S*), reticulocalbin 3 (*RCN3*), *HCK*, and secretory leukocyte peptidase inhibitor (*SLPI*) (Figure 5E).

The diagnostic performance of these six candidate biomarkers was validated using ROC curve analysis. In the

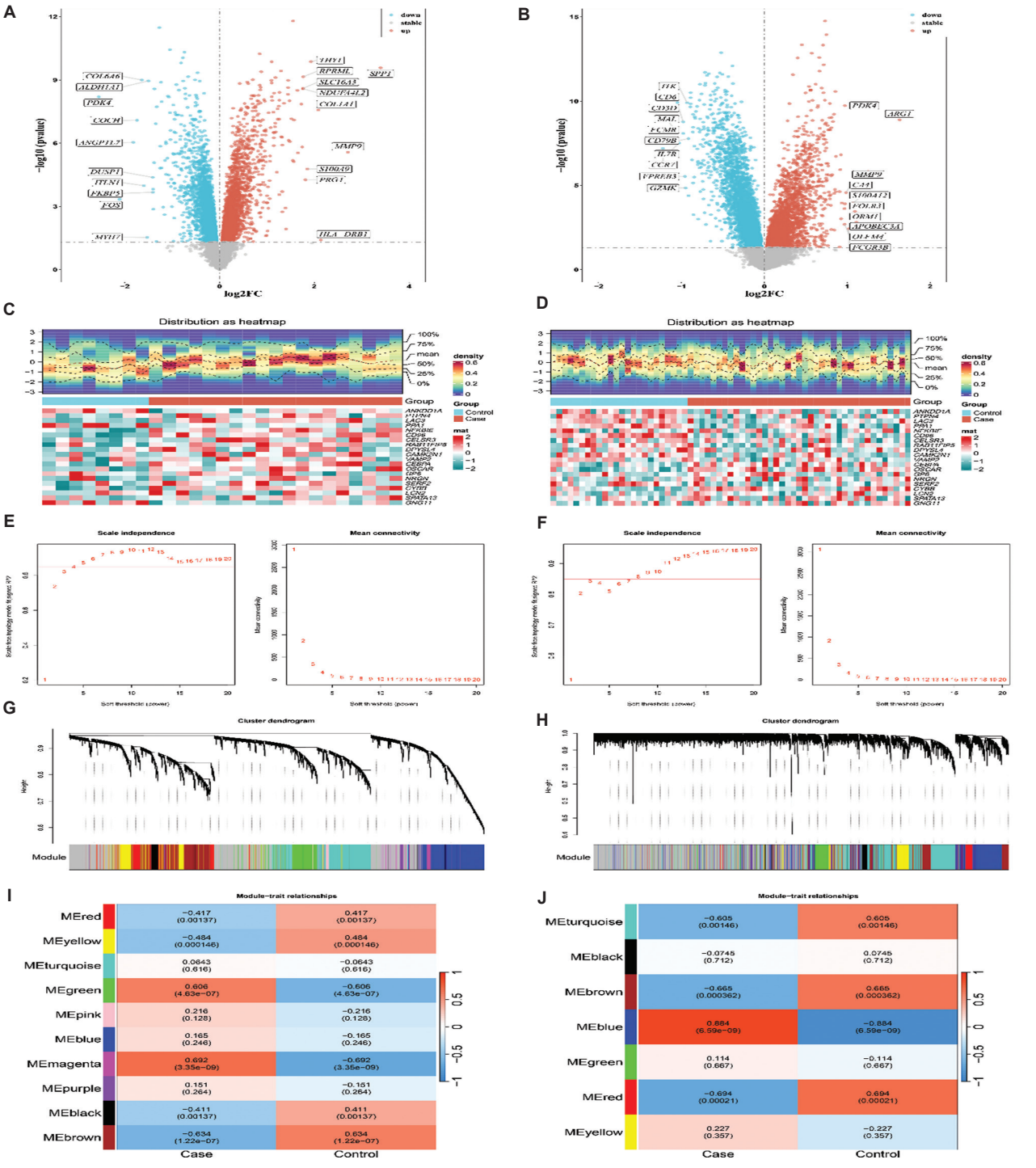

Figure 3. Characterization of differentially expressed genes (DEGs) and weighted gene co-expression network analysis (WGCNA) in ischemic stroke (IHS) and calcific aortic valve stenosis (CAVS). (A) Volcano plot of DEGs in IHS. Upregulated and downregulated genes are presented as red and blue dots, respectively. (B) Volcano plot of DEGs in CAVS. Upregulated and downregulated genes are presented as red and blue dots, respectively. (C) Heatmap of DEGs in IHS. Red and blue represent high and low relative gene expression levels, respectively. (D) Heatmap of DEGs in CAVS. Red and blue represent high and low relative gene expression levels, respectively. (E) Scale-free topology analysis for IHS to determine the optimal soft-thresholding power (β = 5) based on the average connectivity and scale independence. (F) Scale-free topology analysis for CAVS to determine the optimal soft-thresholding power (β = 8) based on the average connectivity and scale independence. (G) Network heatmap showing the gene dendrogram and module eigengenes in IHS. (H) Network heatmap showing the gene dendrogram and module eigengenes in CAVS. (I) Heatmap revealing the correlation (top) and *p*-value (bottom) between module eigengenes and IHS status. (J) Heatmap revealing the correlation (top) and *p*-value (bottom) between module eigengenes and CAVS status.

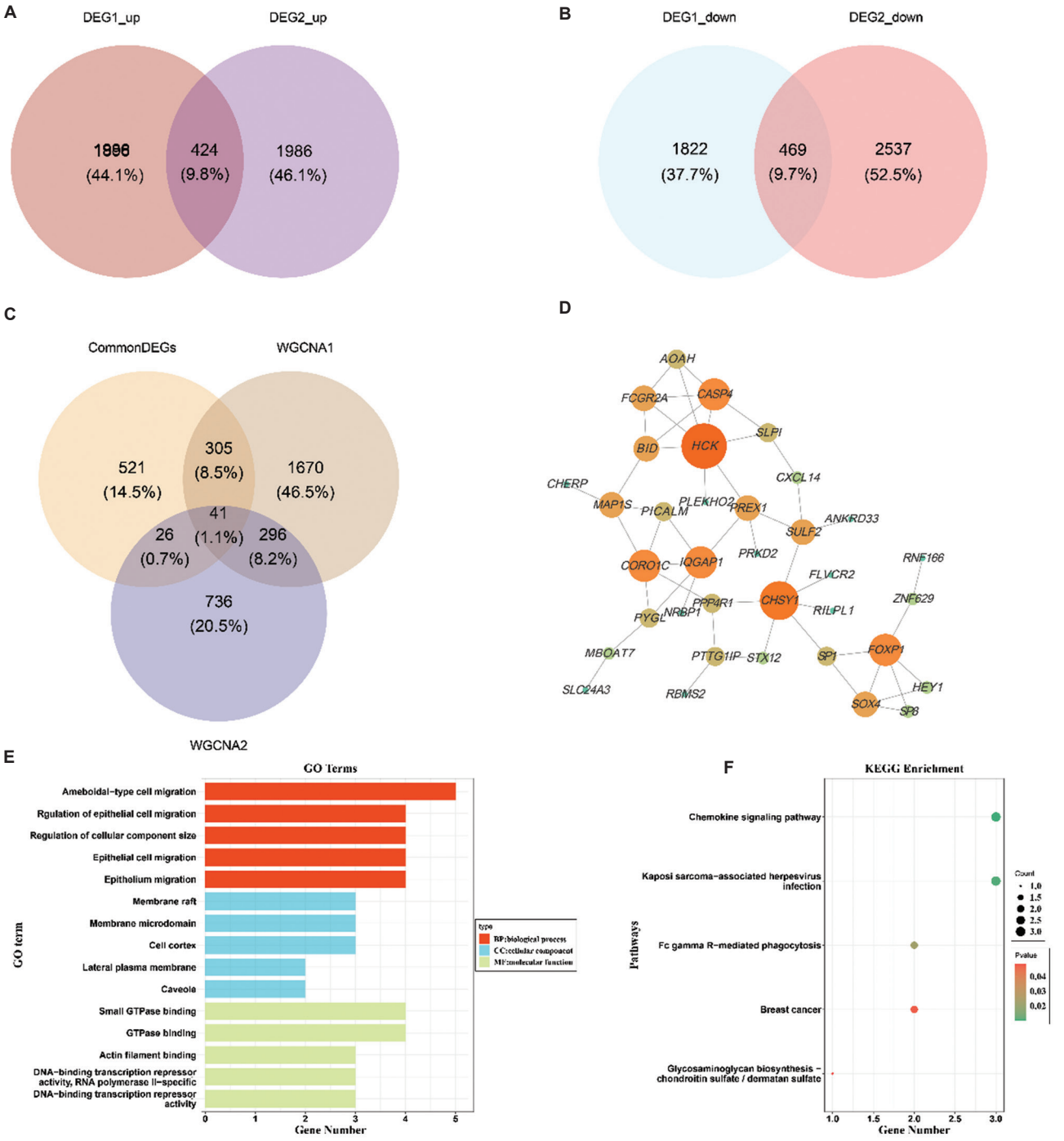

Figure 4. Acquisition, functional enrichment, and protein–protein interaction (PPI) network analysis of key genes. (A) Venn diagram showing the overlap between upregulated differentially expressed genes (DEGs) in ischemic stroke (IHS) and upregulated DEGs in calcific aortic valve stenosis (CAVS), and the number of co-expressed genes. (B) Venn diagram showing the overlap between downregulated DEGs in IHS and downregulated DEGs in CAVS, and the number of co-expressed genes. (C) Venn diagram showing the overlap between key module genes and common DEGs, and the number of key genes. (D) PPI network of the key genes. (E) Gene Ontology functional enrichment analysis of the key genes. (F) Bubble plots depicting Kyoto Encyclopedia of Genes and Genomes pathway enrichment of the key genes.

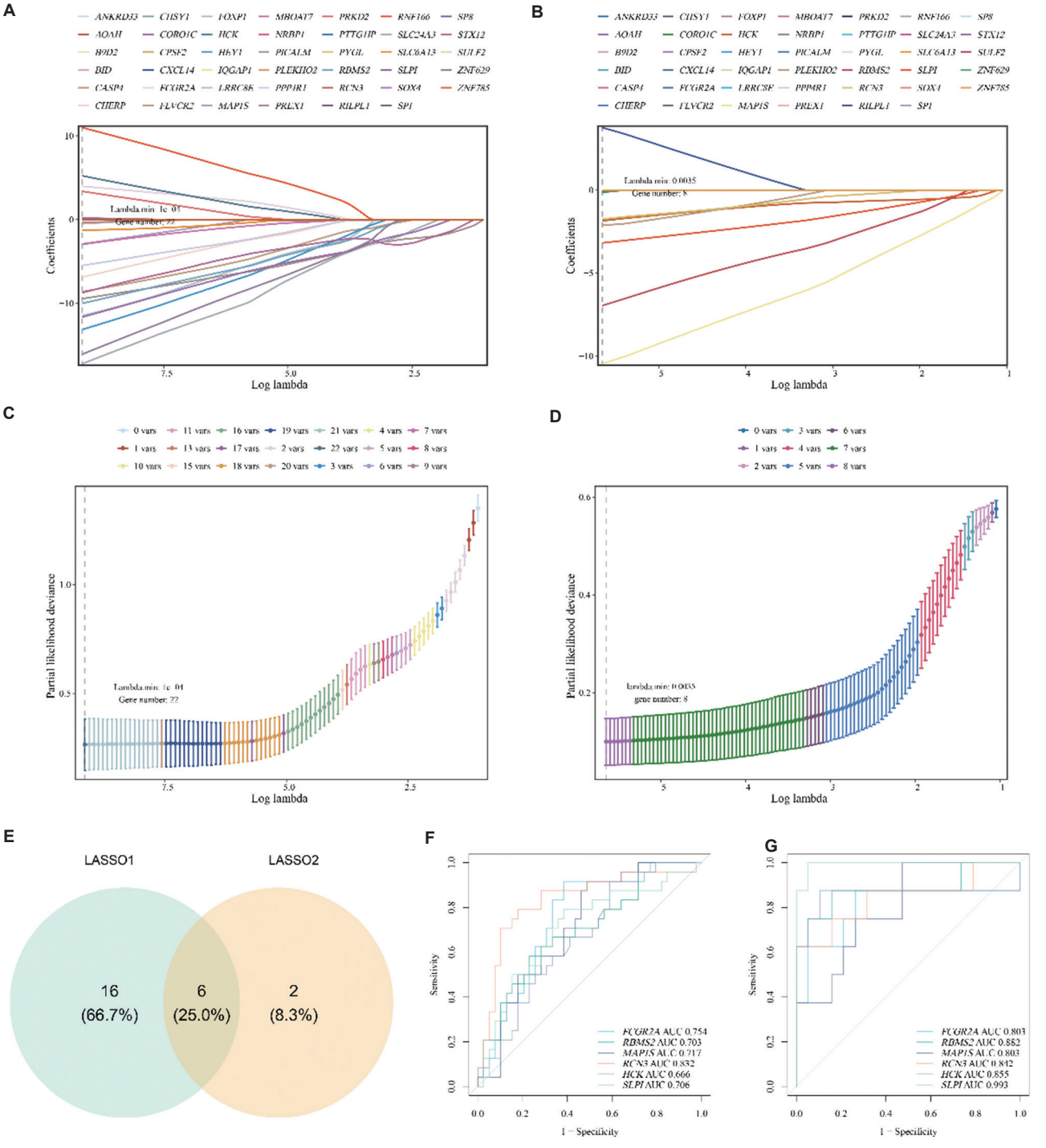

Figure 5. Screening and identification of diagnostic biomarkers for ischemic stroke (IHS) and calcific aortic valve stenosis (CAVS). (A) Least absolute shrinkage and selection operator (LASSO) coefficient profiles of candidate genes for IHS. (B) LASSO coefficient profiles of candidate genes for CAVS. (C) Optimal lambda (λ) values for diagnostic biomarkers in IHS identified by LASSO logistic regression. (D) Optimal λ values for diagnostic biomarkers in CAVS identified by LASSO logistic regression. (E) Venn diagram showing the overlap of common biomarker genes between IHS and CAVS identified by the LASSO logistic regression algorithm. (F) Receiver operating characteristic (ROC) curves of candidate biomarkers in the IHS training set. (G) ROC curves of candidate biomarkers in the CAVS training set.
Abbreviation: AUC: Area under the curve.

IHS training dataset, all six genes exhibited AUC values >0.6 (AUC_{FCGR2A} = 0.754, AUC_{RBMS2} = 0.703, AUC_{MAP1S} = 0.717, AUC_{RCN3} = 0.832, AUC_{HCK} = 0.666, and AUC_{SLPI} = 0.706) (Figure 5F). In the corresponding validation dataset, all six genes demonstrated AUC values exceeding 0.7 (AUC_{FCGR2A} = 0.73, AUC_{RBMS2} = 0.708, AUC_{MAP1S} = 0.888, AUC_{RCN3} = 0.804, AUC_{HCK} = 0.749, and AUC_{SLPI} = 0.858) (Figure A1A). Similarly, in the CAVS training dataset, all six biomarkers achieved AUC values above 0.8 (AUC_{FCGR2A} = 0.803, AUC_{RBMS2} = 0.882, AUC_{MAP1S} = 0.803, AUC_{RCN3} = 0.842, AUC_{HCK} = 0.855, and AUC_{SLPI} = 0.993) (Figure 5G). Consistently, AUC values in the validation set were also all >0.8 for all six genes (AUC_{FCGR2A} = 0.8, AUC_{RBMS2} = 0.84, AUC_{MAP1S} = 0.93, AUC_{RCN3} = 0.8, AUC_{HCK} = 0.9, and AUC_{SLPI} = 0.85) (Figure A1B). Collectively, *FCGR2A*, *RBMS2*, *MAP1S*, *RCN3*, *HCK*, and *SLPI* were identified as diagnostic biomarkers for both IHS and CAVS. Figure A2 shows the expression patterns of these six biomarkers, all of which were significantly differentially expressed across training and validation datasets for both IHS and CAVS.

3.6. ANN models and co-expression networks for biomarkers

Based on the six identified biomarkers, we constructed ANN models and categorized gene expression data into case and control groups (Figure 6A and B). Our prediction model, which utilized six biomarkers, exhibited good discrimination based on ROC curve analysis. Specifically, for IHS, the AUC values were 0.974 in the training dataset and 0.888 in the validation dataset. Similarly, for CAVS, the AUC was 1.00 in the training dataset and 0.95 in the validation dataset (Figure 6C and D).

To obtain a deeper understanding of the interactions among the six biomarkers, genes with established associations with these biomarkers were examined. Analysis of the biomarker co-expression network constructed using GeneMANIA revealed that these genes were mainly associated with immunomodulatory cell surface receptor signaling pathways involved in phagocytosis, the Fc receptor signaling pathway, Fc-gamma receptor signaling pathway, and Fc receptor-mediated stimulatory signaling pathway (Figure 6E).

3.7. Analysis of the immune characteristics of IHS and CAVS

Pathway exploration analysis revealed that the immune system plays a crucial role in both IHS and CAVS. To quantitatively assess immune cell infiltration, ssGSEA was used to estimate the relative abundance of 28 immune cell phenotypes in IHS and CAVS samples. In both IHS and CAVS, we observed notable variations in most immune cell subsets when comparing disease samples with normal controls (Figure 7A and B). Particularly, activated B cells, activated CD8 T cells, activated dendritic cells, central memory CD8 T cells, effector memory CD8 T cells, eosinophils, gamma delta T cells, macrophages, natural killer cells, plasmacytoid dendritic cells, and regulatory T cells were identified as common differentially infiltrated immune cell types in both diseases. Figure 7C and D illustrate the correlation between the 28 immune cells and six biomarkers in both IHS and CAVS. Among the 11 immune cell types commonly differentiated in both diseases, activated dendritic cells were significantly and positively correlated with all six biomarkers in both IHS and CAVS.

3.8. Screening results for small-molecule drugs

Potential therapeutic agents targeting *FCGR2A* and *HCK* were screened using the DrugBank database. Drug–gene interaction analysis revealed that *FCGR2A* and *HCK* were associated with multiple candidate drugs (Table A2). Drugs corresponding to *FCGR2A* included cetuximab, etanercept, human immunoglobulin G, abciximab, alemtuzumab, daclizumab, sarilumab, catumaxomab, and bevacizumab. Drugs associated with *HCK* included 1-*Tert*-butyl-3-P-tolyl-1h-pyrazolo [3,4-D] pyrimidin-4-ylamine, phosphonotyrosine, quercetin, fostamatinib, bosutinib, doramapimod, and PP-121.

4. Discussion

In this study, we first examined the bidirectional causal link between IHS and CAVS using MR analysis. Our results suggest that IHS causally promotes the development of CAVS, whereas CAVS does not exert a significant causal effect on IHS. We further explored shared mechanisms and potential diagnostic biomarkers for both diseases using bioinformatics analyses. Our results showed that multiple immune-related pathways may represent common pathogenic mechanisms underlying IHS and CAVS. Moreover, *FCGR2A*, *RBMS2*, *MAP1S*, *RCN3*, *HCK*, and *SLPI* were identified as shared diagnostic biomarkers for both IHS and CAVS. Based on these six biomarkers, an ANN–based diagnostic model was developed to ensure an accurate diagnosis for both diseases. The identified pathways and biomarkers offer valuable insights into the shared pathogenesis of these diseases and establish a theoretical foundation for future research.

Previous clinical investigations examining the relationship between IHS and CAVS have yielded conflicting results.[17,22,50] Clinical studies reported no significant increase in stroke incidence among patients with CAVS,[21,22,51] which is consistent with our findings. In contrast, other studies indicated that patients with AVS are at a significantly higher risk of developing IHS.[17,50,52] However, conclusions

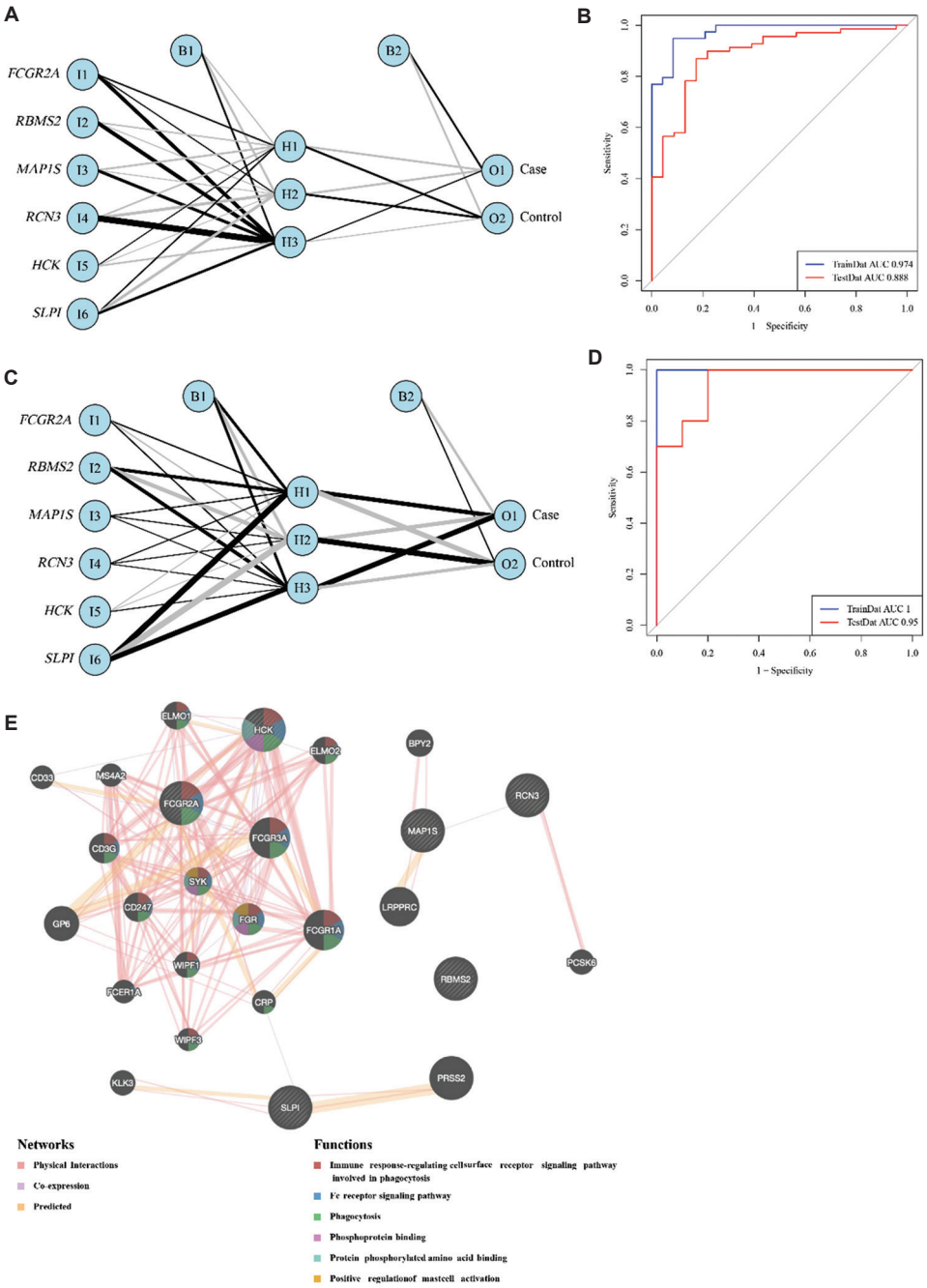

Figure 6. Construction of artificial neural network (ANN) models and co-expression network of biomarkers. (A) ANN models for ischemic stroke (IHS). (B) ANN models for calcific aortic valve stenosis (CAVS). (C) Receiver operating characteristic (ROC) curves of the ANN model in the IHS training and validation sets. (D) ROC curves of ANN models in the CAVS training and validation sets. (E) Biomarker co-expression network using GeneMANIA analysis.

drawn from observational and prospective clinical studies may be influenced by confounding factors or covariates and do not necessarily imply causality. Variations in study outcomes may be attributable to differences in race, age, sex, and comorbid conditions. By leveraging MR analysis, we confirmed that IHS is a risk factor for CAVS with no evidence supporting a reverse causal relationship between the two diseases. This MR approach reduces confounding and reverse causation relative to conventional observational analyses and provides complementary evidence when randomized controlled trials are impractical.

Immune and inflammatory responses appear to play a pivotal role in linking IHS and CAVS. Pathophysiological

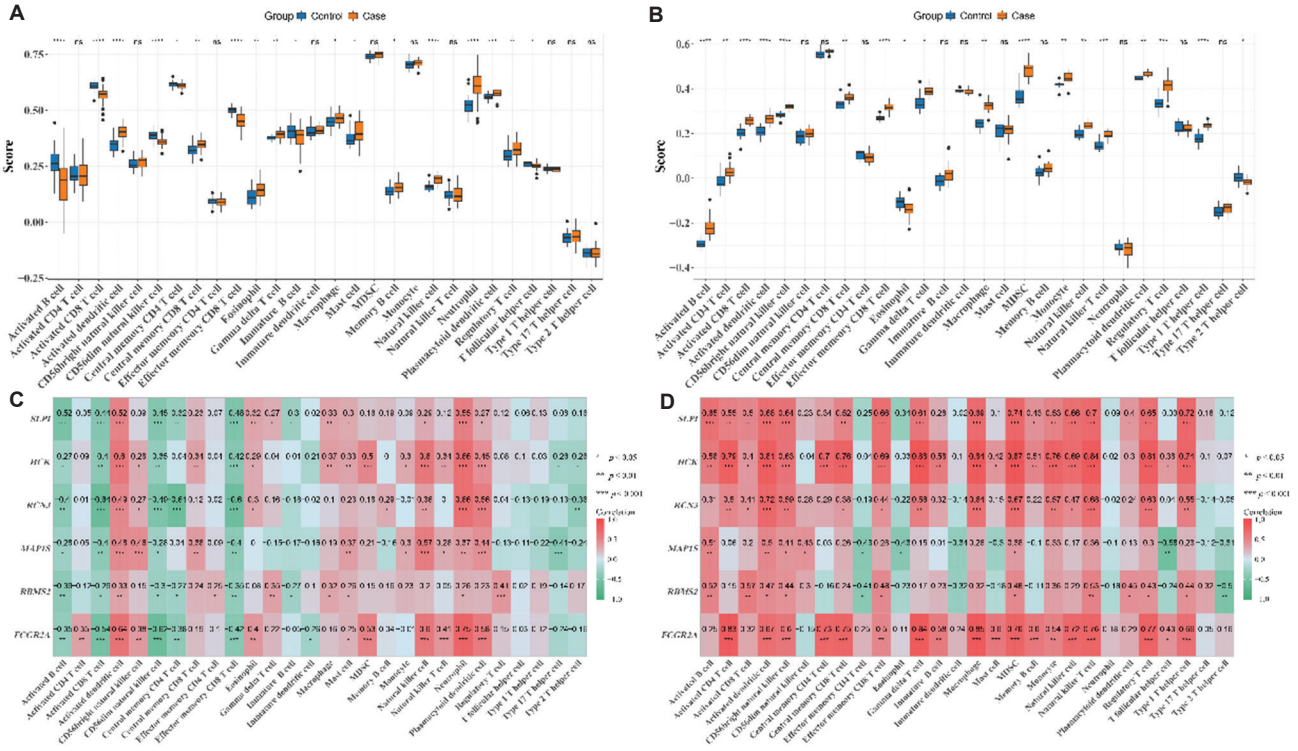

Figure 7. Immune infiltration analysis in ischemic stroke (IHS) and calcific aortic valve stenosis (CAVS). (A) Box plot showing the expression levels of distinct immune cell subsets in IHS. (B) Box plot showing the expression levels of different immune cell subsets in CAVS. (C) Correlation heatmap illustrating the relationships between biomarkers and immune cell subsets in IHS. (D) Correlation heatmap illustrating the relationships between biomarkers and immune cell subsets in CAVS.
Notes: ns denotes $p > 0.05$; * denotes $p \leq 0.05$; ** denotes $p \leq 0.01$; *** denotes $p \leq 0.001$; and **** denotes $p \leq 0.0001$.

changes encompass ionic imbalance, neuroinflammation, and abnormal immune cell activation. Interleukins (ILs) play dual roles in IHS by facilitating the activation, proliferation, differentiation, and inflammatory response of T and B cells by transmitting information and regulating immune cell activity.[53] Elevated levels of IL-1β, IL-6, IL-8, and IL-17 have been reported in patients with IHS,[53] and inflammatory mediators have been extensively studied as potential prognostic indicators and therapeutic targets.[54] Inflammatory cytokines are key drivers of AVC disease,[55] while the inflammatory response plays a primary role in the early stages of CAVS.[56] Increased levels of specific inflammatory proteins have been associated with AVC severity and progression.[57,58] MR analyses suggested that the elevated levels of some inflammatory proteins are associated with an increased risk of CAVS.[3] For example, IL-8 promotes valvular calcification through CXC motif chemokine receptor 2–dependent and matrix metalloproteinase 12–dependent mechanisms.[59] IL-17A triggers inflammation in the endothelial lining of the aortic valve,[60] and IL-1β promotes the expression of matrix metalloproteinases and cellular proliferation in CAVS.[61] In addition, localized inflammation also causes abnormal blood vessel formation, further accelerating CAVS progression.[62] In this study, 41 key genes shared by IHS and CAVS were predominantly enriched in immune- and inflammation-related pathways, reinforcing the notion that immune-inflammatory mechanisms underlie IHS-related CAVS.

Alterations in immune cell populations appear to significantly influence the association between IHS and CAVS. Our results showed that several immune cells, such as activated dendritic cells, central memory $CD8^+$ T cells, gamma delta T cells, macrophages, natural killer cells, plasmacytoid dendritic cells, and regulatory T cells, were highly expressed in IHS and CAVS. Macrophages, in particular, have emerged as the predominant immune cell type involved in numerous valvular heart diseases.[63] Upon tissue infiltration, macrophages secrete inflammatory cytokines, including tumor necrosis factor-α, IL-1β, and transforming growth factor-β, resulting in inflammation of the cardiac valves. Additionally, tumor necrosis factor-α and transforming growth factor-β also activate valve interstitial cells and stimulate alkaline phosphatase synthesis, ultimately promoting valvular calcification.[64,65] Activated local macrophages and T lymphocytes (CD4+

and CD8+) within the calcified valve further increased the production of proinflammatory factors.[66] In patients with CAVS, inflammatory macrophages promote valve interstitial cell calcification in a cathepsin-S-dependent manner.[67] Monocytes and macrophages undergo calcification by secreting tumor necrosis factor.[68] We also explored the correlations between immune cell subsets and the six identified biomarkers to gain insights into the immune-related mechanisms underlying IHS and CAVS pathogenesis.

We identified six biomarker genes, *FCGR2A*, *RBMS2*, *MAP1S*, *RCN3*, *HCK*, and *SLPI*, and determined the association of these biomarkers with IHS and CAVS. The expression levels of *FCGR2A*, *RBMS2*, *MAP1S*, *RCN3*, *HCK*, and *SLPI* were significantly higher in both the IHS and CAVS groups compared with those in the control groups. The diagnostic model incorporating these six biomarkers demonstrated strong predictive performance for both conditions. *FCGR2A* encodes a protein belonging to the immunoglobulin Fc receptor family.[69] Genetic variations in *FCGR2A* have been shown to correlate with susceptibility to inflammation-related diseases,[70,71] including IHS[72,73] and CAVS.[74] *RBMS2* is associated with tumor suppressor activity and participates in essential cellular mechanisms related to cell growth and programmed cell death (apoptosis).[75] *MAP1S* functions as a linker between mitochondria and microtubules, facilitating intracellular transport and connecting autophagy mechanisms with microtubules and mitochondria, thereby influencing the biogenesis and degradation of autophagosomes.[76] *RCN3* plays a crucial role in protein biosynthesis and has emerged as a target for various cancer-related treatment interventions.[77] In *RCN3* knockdown cells, genes involved in translation, ribosomal function, and cytokine signaling are downregulated, whereas genes associated with immune response, stem cell differentiation, and extracellular matrix are upregulated.[77] *HCK*, a member of the SRC family of cytoplasmic tyrosine kinases, is recognized as a therapeutic target for immune and cancer cells.[78] Qiao *et al*. identified *HCK* as a potential candidate biomarker for AVC, which is consistent with our findings.[79] *SLPI*, a member of the whey acidic protein family, plays an important role in suppressing human neutrophil-derived serine proteases[80,81] and is involved in host defense, inflammatory regulation, and cell fate determination.[81] Zhu *et al*.[82] reported that *SLPI* may serve as a potential diagnostic biomarker for AVC. In conclusion, *FCGR2A*, *RBMS2*, *MAP1S*, *RCN3*, *HCK*, and *SLPI* are suitable biomarkers for distinguishing calcific pathology. Furthermore, we screened potential small-molecule drugs targeting these biomarkers, providing further insight into the diagnosis and treatment of IHS and CAVS.

This study has several strengths. First, using MR analysis, we confirmed that IHS is a risk factor for CAVS and found no evidence of reverse causality, thereby providing a robust causal framework for future clinical investigations. Second, we identified six shared biomarkers between IHS and CAVS, and a diagnostic model based on these biomarkers exhibited strong predictive performance for both conditions. Finally, our findings highlight the central role of inflammation and immune responses in the pathogenesis of IHS and CAVS, providing a deeper understanding of their shared molecular mechanisms and pathways.

Nevertheless, this study has several limitations. The MR analysis was based exclusively on data from populations of European ancestry, without stratification by sex, race, or other demographic factors, which may limit the generalizability of the findings to other populations. Furthermore, the conclusions were derived primarily from computational predictions of publicly available datasets related to IHS and CAVS. Further experimental and clinical validation is imperative to ascertain the biological functions of the investigated biomarkers and delineate their underlying signaling pathways.

5. Conclusion

We conducted MR analysis to investigate the causal link between IHS and CAVS. MR analysis suggested that genetically predicted IHS is associated with increased risk of CAVS, whereas CAVS does not exert a significant causal effect on IHS. In addition, we identified six biomarkers shared by both IHS and CAVS. The diagnostic model incorporating these biomarkers demonstrated strong predictive performance for both conditions. IHS and CAVS were associated with multiple immune-inflammatory pathways, providing a mechanistic foundation for future research and warranting further evaluations in both experimental and clinical settings.

Acknowledgments

Ischemic stroke data used for MR analysis were obtained from the Integrative Epidemiology Unit Open Genome-Wide Association Study (GWAS) database (https://gwas.mrcieu.ac.uk/). Summary statistics for the GWAS of calcific aortic valve stenosis for MR analysis were obtained from the FinnGen database (https://r10.finngen.fi/). We thank all researchers for sharing these data.

Funding

This study was supported by Guangzhou Health and Wellness Commission (Grant number: 20221A011108), Guangzhou Science and Technology Plan Project

(Grant number: 202201011779), and Key Laboratory of Guangdong Higher Education Institutes (2021KSYS009).

Conflict of interest

The authors declare no competing interests.

Author contributions

Conceptualization: Rensheng Song
Formal analysis: Weihong Jin, Huiling Zheng
Investigation: Sha He, Haoda Li
Methodology: Junhui Zhong
Writing–original draft: Hongli Xian, Yan Hu
Writing–review & editing: Minghua Zhang

Ethics approval and consent to participate

Not applicable

Consent for publication

Not applicable

Availability of data

The data that support the findings of this study are available from the corresponding author upon reasonable request.

References

1. Eveborn GW, Schirmer H, Heggelund G, Lunde P, Rasmussen K. The evolving epidemiology of valvular aortic stenosis. The Tromsø study. *Heart*. 2013;99(6):396-400.

   doi: 10.1136/heartjnl-2012-302265

2. Pan W, Zhou D, Cheng L, Shu X, Ge J. Candidates for transcatheter aortic valve implantation may be fewer in China. *Int J Cardiol*. 2013;168(5):e133-e134.

   doi: 10.1016/j.ijcard.2013.08.028

3. Lin R, Zhu Y, Chen W, Wang Z, Wang Y, Du J. Identification of circulating inflammatory proteins associated with calcific aortic valve stenosis by multiplex analysis. *Cardiovasc Toxicol*. 2024;24(5):499-512.

   doi: 10.1007/s12012-024-09854-5

4. Peeters FE, Meex SJ, Dweck MR, *et al*. Calcific aortic valve stenosis: Hard disease in the heart: A biomolecular approach towards diagnosis and treatment. *Eur Heart J*. 2018;39(28):2618-2624.

   doi: 10.1093/eurheartj/ehx653

5. Carabello BA, Paulus WJ. Aortic stenosis. *Lancet*. 2009;373(9667):956-966.

   doi: 10.1016/s0140-6736(09)60211-7

6. Yadgir S, Johnson CO, Aboyans V, *et al*. Global, regional, and national burden of calcific aortic valve and degenerative mitral valve diseases, 1990-2017. *Circulation*. 2020, 141(21):1670-1680.

   doi: 10.1161/circulationaha.119.043391

7. Otto CM, Prendergast B. Aortic-valve stenosis--from patients at risk to severe valve obstruction. *N Engl J Med*. 2014;371(8):744-756.

   doi: 10.1056/nejmra1313875

8. Baumgartner H, Falk V, Bax JJ, *et al*. 2017 ESC/EACTS guidelines for the management of valvular heart disease. *Kardiol Pol*. 2018;76(1):1-62.

   doi: 10.5603/kp.2018.0013

9. Haakenstad A, Yearwood JA, Fullman N, *et al*. Assessing performance of the healthcare access and quality index, overall and by select age groups, for 204 countries and territories, 1990-2019: A systematic analysis from the global burden of disease study 2019. *Lancet Glob Health*. 2022;10(12):e1715-e1743.

   doi: 10.1016/s2214-109x(22)00429-6

10. Donkor ES. Stroke in the 21st century: A snapshot of the burden, epidemiology, and quality of life. *Stroke Res Treat*. 2018;2018:3238165.

    doi: 10.1155/2018/3238165

11. Herpich F, Rincon F. Management of acute ischemic stroke. *Crit Care Med*. 2020;48(11):1654-1663.

    doi: 10.1097/ccm.0000000000004597

12. Powers WJ. Acute ischemic stroke. *N Engl J Med*. 2020;383(3):252-260.

    doi: 10.1056/nejmcp1917030

13. Li Y, Lu J, Wang J, *et al*. Inflammatory cytokines and risk of ischemic stroke: A mendelian randomization study. *Front Pharmacol*. 2021;12:779899.

    doi: 10.3389/fphar.2021.779899

14. Kapadia SR, Makkar R, Leon M, *et al*. Cerebral embolic protection during transcatheter aortic-valve replacement. *N Engl J Med*. 2022;387(14):1253-1263.

    doi: 10.1056/nejmoa2204961

15. Blankenberg S, Seiffert M, Vonthein R, *et al*. Transcatheter or surgical treatment of aortic-valve stenosis. *N Engl J Med*. 2024;390(17):1572-1583.

    doi: 10.1056/nejmoa2400685

16. Daneault B, Kirtane AJ, Kodali SK, *et al*. Stroke associated with surgical and transcatheter treatment of aortic stenosis: A comprehensive review. *J Am Coll Cardiol*. 2011;58(21):2143-2150.

    doi: 10.1016/j.jacc.2011.08.024

17. Andreasen C, Gislason GH, Køber L, *et al*. Incidence of ischemic stroke in individuals with and without aortic valve stenosis: A Danish retrospective cohort study. *Stroke*.

2020;51(5):1364-1371.

doi: 10.1161/strokeaha.119.028389

18. Wilson JH, Cranley JJ. Recurrent calcium emboli in a patient with aortic stenosis. *Chest*. 1989;96(6):1433-1434.

doi: 10.1378/chest.96.6.1433

19. Ito A, Iwata S, Tamura S, *et al*. Prevalence and risk factors of silent brain infarction in patients with aortic stenosis. *Cerebrovasc Dis Extra*. 2020;10(3):116-123.

doi: 10.1159/000510438

20. Gupta A, Giambrone AE, Gialdini G, *et al*. Silent brain infarction and risk of future stroke: A systematic review and meta-analysis. *Stroke*. 2016;47(3):719-725.

doi: 10.1161/strokeaha.115.011889

21. Boon A, Lodder J, Cheriex E, Kessels F. Risk of stroke in a cohort of 815 patients with calcification of the aortic valve with or without stenosis. *Stroke*. 1996;27(5):847-851.

doi: 10.1161/01.str.27.5.847

22. Bos D, Bozorgpourniazi A, Mutlu U, *et al*. Aortic valve calcification and risk of stroke: The rotterdam study. *Stroke*. 2016;47(11):2859-2861.

doi: 10.1161/strokeaha.116.015200

23. Sekula P, Del Greco MF, Pattaro C, Köttgen A. Mendelian randomization as an approach to assess causality using observational data. *J Am Soc Nephrol.* 2016;27(11):3253-3265.

doi: 10.1681/asn.2016010098

24. Swanson SA, Tiemeier H, Ikram MA, Hernán MA. Nature as a trialist?: Deconstructing the analogy between mendelian randomization and randomized trials. *Epidemiology*. 2017;28(5):653-659.

doi: 10.1097/ede.0000000000000699

25. Fernández-Ruiz I. Artificial intelligence to improve the diagnosis of cardiovascular diseases. *Nat Rev Cardiol*. 2019;16(3):133.

doi: 10.1038/s41569-019-0158-5

26. Bertsimas D, Mingardi L, Stellato B. Machine learning for real-time heart disease prediction. *IEEE J Biomed Health Inform*. 2021;25(9):3627-3637.

doi: 10.1109/jbhi.2021.3066347

27. Kurki MI, Karjalainen J, Palta P, *et al*. FinnGen provides genetic insights from a well-phenotyped isolated population. *Nature*. 2023;613(7944):508-518.

doi: 10.1038/s41586-022-05473-8

28. Lawlor DA, Harbord RM, Sterne JA, Timpson N, Davey Smith G. Mendelian randomization: Using genes as instruments for making causal inferences in epidemiology. *Stat Med*. 2008;27(8):1133-1163.

doi: 10.1002/sim.3034

29. Swerdlow DI, Kuchenbaecker KB, Shah S, *et al*. Selecting instruments for Mendelian randomization in the wake of genome-wide association studies. *Int J Epidemiol*. 2016;45(5):1600-1616.

doi: 10.1093/ije/dyw088

30. Ouyang F, Yuan P, Ju Y, Chen W, Peng Z, Xu H. Alzheimer's disease as a causal risk factor for diabetic retinopathy: A Mendelian randomization study. *Front Endocrinol (Lausanne)*. 2024;15:1340608.

doi: 10.3389/fendo.2024.1340608

31. Wu H, Wang H, Liu D, Liu Z, Zhang W. Mendelian randomization analyses of associations between breast cancer and bone mineral density. *Sci Rep.* 2023;13(1):1721.

doi: 10.1038/s41598-023-28899-0

32. Olwi DI, Kaisinger LR, Kentistou KA, *et al*. Likely causal effects of insulin resistance and IGF-1 bioaction on childhood and adult adiposity: A Mendelian randomization study. *Int J Obes (Lond)*. 2024;48(11):1650-1655.

doi: 10.1038/s41366-024-01605-4

33. Hemani G, Tilling K, Davey Smith G. Orienting the causal relationship between imprecisely measured traits using GWAS summary data. *PLoS Genet*. 2017;13(11):e1007081.

doi: 10.1371/journal.pgen.1007081

34. Hemani G, Zheng J, Elsworth B, *et al*. The MR-Base platform supports systematic causal inference across the human phenome. *Elife*. 2018;7:e34408.

doi: 10.7554/eLife.34408

35. Burgess S, Davey Smith G, Davies NM, *et al*. Guidelines for performing Mendelian randomization investigations: Update for summer 2023. *Wellcome Open Res*. 2023;4:186.

doi: 10.12688/wellcomeopenres.15555.3

36. Greco MF, Minelli C, Sheehan NA, Thompson JR. Detecting pleiotropy in Mendelian randomisation studies with summary data and a continuous outcome. *Stat Med*. 2015;34(21):2926-2940.

doi: 10.1002/sim.6522

37. Bowden J, Davey Smith G, Burgess S. Mendelian randomization with invalid instruments: Effect estimation and bias detection through Egger regression. *Int J Epidemiol*. 2015;44(2):512-525.

doi: 10.1093/ije/dyv080

38. Verbanck M, Chen CY, Neale B, Do R. Detection of widespread horizontal pleiotropy in causal relationships inferred from Mendelian randomization between complex traits and diseases. *Nat Genet*. 2018;50(5):693-698.

doi: 10.1038/s41588-018-0099-7

39. Ritchie ME, Phipson B, Wu D, *et al*. Limma powers differential expression analyses for RNA-sequencing and

microarray studies. *Nucleic Acids Res*. 2015;43(7):e47.

doi: 10.1093/nar/gkv007

40. Langfelder P, Horvath S. WGCNA: An R package for weighted correlation network analysis. *BMC Bioinformatics*. 2008;9:559.

doi: 10.1186/1471-2105-9-559

41. Yu G, Wang LG, Han Y, He QY. Clusterprofiler: An R package for comparing biological themes among gene clusters. *OMICS*. 2012;16(5):284-287.

doi: 10.1089/omi.2011.0118

42. Szklarczyk D, Gable AL, Lyon D, *et al*. STRING v11: Protein-protein association networks with increased coverage, supporting functional discovery in genome-wide experimental datasets. *Nucleic Acids Res*. 2019;47(D1):D607-D613.

doi: 10.1093/nar/gky1131

43. Shannon P, Markiel A, Ozier O, *et al*. Cytoscape: A software environment for integrated models of biomolecular interaction networks. *Genome Res*. 2003;13(11):2498-2504.

doi: 10.1101/gr.1239303

44. Frost HR, Amos CI. Gene set selection via LASSO penalized regression (SLPR). *Nucleic Acids Res*. 2017;45(12):e114.

doi: 10.1093/nar/gkx291

45. Friedman J, Hastie T, Tibshirani R. Regularization paths for generalized linear models via coordinate descent. *J Stat Softw*. 2010;33(1):1-22.

doi: 10.18637/jss.v033.i01

46. Rosenblatt F. The perceptron: A probabilistic model for information storage and organization in the brain. *Psychol Rev*. 1958;65(6):386-408.

doi: 10.1037/h0042519

47. Warde-Farley D, Donaldson SL, Comes O, *et al*. The GeneMANIA prediction server: Biological network integration for gene prioritization and predicting gene function. *Nucleic Acids Res*. 2010;38:W214-W220.

doi: 10.1093/nar/gkq537

48. Barbie DA, Tamayo P, Boehm JS, *et al*. Systematic RNA interference reveals that oncogenic KRAS-driven cancers require TBK1. *Nature*. 2009;462(7269):108-112.

doi: 10.1038/nature08460

49. Knox C, Wilson M, Klinger CM, *et al*. DrugBank 6.0: The DrugBank knowledgebase for 2024. *Nucleic Acids Res*. 2024;52(D1):D1265-D1275.

doi: 10.1093/nar/gkad976

50. Zhang D, Dai X, Wang C, *et al*. Aortic valve calcification and risk of stroke: A systematic review and meta-analysis. *J Clin Neurosci*. 2018;55:32-37.

doi: 10.1016/j.jocn.2018.07.016

51. Cosmi JE, Kort S, Tunick PA, *et al*. The risk of the development of aortic stenosis in patients with "benign" aortic valve thickening. *Arch Intern Med*. 2002;162(20):2345-2347.

doi: 10.1001/archinte.162.20.2345

52. Makkar RR, Yoon SH, Leon MB, *et al*. Association between transcatheter aortic valve replacement for bicuspid vs tricuspid aortic stenosis and mortality or stroke. *JAMA*. 2019;321(22):2193-2202.

doi: 10.1001/jama.2019.7108

53. Zhu H, Hu S, Li Y, *et al*. Interleukins and ischemic stroke. *Front Immunol*. 2022;13:828447.

doi: 10.3389/fimmu.2022.828447

54. Tirandi A, Sgura C, Carbone F, Montecucco F, Liberale L. Inflammatory biomarkers of ischemic stroke. *Intern Emerg Med*. 2023;18(3):723-732.

doi: 10.1007/s11739-023-03201-2

55. Yu Chen H, Dina C, Small AM, *et al*. Dyslipidemia, inflammation, calcification, and adiposity in aortic stenosis: A genome-wide study. *Eur Heart J*. 2023;44(21):1927-1939.

doi: 10.1093/eurheartj/ehad142

56. Driscoll K, Cruz AD, Butcher JT. Inflammatory and biomechanical drivers of endothelial-interstitial interactions in calcific aortic valve disease. *Circ Res*. 2021;128(9):1344-1370.

doi: 10.1161/circresaha.121.318011

57. Galante A, Pietroiusti A, Vellini M, *et al*. C-reactive protein is increased in patients with degenerative aortic valvular stenosis. *J Am Coll Cardiol*. 2001;38(4):1078-1082.

doi: 10.1016/s0735-1097(01)01484-x

58. Small A, Kiss D, Giri J, *et al*. Biomarkers of calcific aortic valve disease. *Arterioscler Thromb Vasc Biol*. 2017;37(4):623-632.

doi: 10.1161/atvbaha.116.308615

59. Coté N, Mahmut A, Bosse Y, *et al*. Inflammation is associated with the remodeling of calcific aortic valve disease. *Inflammation*. 2013;36(3):573-581.

doi: 10.1007/s10753-012-9579-6

60. Yang Z, Zhang J, Zhu Y, *et al*. IL-17A induces valvular endothelial inflammation and aggravates calcific aortic valve disease. *Biochem Biophys Res Commun*. 2023;672:145-153.

doi: 10.1016/j.bbrc.2023.04.079

61. Kaden JJ, Dempfle CE, Grobholz R, *et al*. Interleukin-1 beta promotes matrix metalloproteinase expression and cell proliferation in calcific aortic valve stenosis. *Atherosclerosis*. 2003;170(2):205-211.

doi: 10.1016/s0021-9150(03)00284-3

62. Conte M, Petraglia L, Campana P, *et al*. The role of inflammation and metabolic risk factors in the pathogenesis

of calcific aortic valve stenosis. *Aging Clin Exp Res*. 2021;33:1765-1770.

doi: 10.1007/s40520-020-01681-2

63. Lee SH, Choi JH. Involvement of immune cell network in aortic valve stenosis: Communication between valvular interstitial cells and immune cells. *Immune Netw*. 2016;16(1):26-32.

doi: 10.4110/in.2016.16.1.26

64. Kaden JJ, Kiliç R, Sarikoç A, *et al*. Tumor necrosis factor alpha promotes an osteoblast-like phenotype in human aortic valve myofibroblasts: A potential regulatory mechanism of valvular calcification. *Int J Mol Med*. 2005;16(5):869-872.

doi: 10.3892/ijmm.16.5.869

65. Parameswaran N, Patial S. Tumor necrosis factor-α signaling in macrophages. *Crit Rev Eukaryot Gene Expr*. 2010;20(2):87-103.

doi: 10.1615/critreveukargeneexpr.v20.i2.10

66. Mathieu P, Bouchareb R, Boulanger MC. Innate and adaptive immunity in calcific aortic valve disease. *J Immunol Res*. 2015;2015:851945.

doi: 10.1155/2015/851945

67. Aikawa E, Aikawa M, Libby P, *et al*. Arterial and aortic valve calcification abolished by elastolytic cathepsin S deficiency in chronic renal disease. *Circulation*. 2009;119(13):1785-1794.

doi: 10.1161/circulationaha.108.827972

68. Goody PR, Hosen MR, Christmann D, *et al*. Aortic valve stenosis: From basic mechanisms to novel therapeutic targets. *Arterioscler Thromb Vasc Biol*. 2020;40(4):885-900.

doi: 10.1161/atvbaha.119.313067

69. Márquez Pete N, Maldonado Montoro MDM, Pérez Ramírez C, *et al*. Influence of the FCGR2A rs1801274 and FCGR3A rs396991 polymorphisms on response to abatacept in patients with rheumatoid arthritis. *J Pers Med*. 2021;11(6):573.

doi: 10.3390/jpm11060573

70. Dai Y, Chen W, Huang J, Cui T. FCGR2A could function as a prognostic marker and correlate with immune infiltration in head and neck squamous cell carcinoma. *Biomed Res Int*. 2021;2021:8874578.

doi: 10.1155/2021/8874578

71. Van Der Meer IM, Witteman JC, Hofman A, Kluft C, De Maat MP. Genetic variation in fcgamma receptor IIa protects against advanced peripheral atherosclerosis. The rotterdam study. *Thromb Haemost*. 2004;92(6):1273-1276.

doi: 10.1160/th04-05-0268

72. Kim YS, Yoo JH, Lee BC. Susceptibility for ischemic stroke in Korean population is associated with polymorphisms of the Fc gamma receptor IIA. *Blood Coagul Fibrinolysis*. 2009;20(5):353-357.

doi: 10.1097/mbc.0b013e32832a86fe

73. Lee BC, Lee H, Park HK, Yang JS, Chung JH. Susceptibility for ischemic stroke in four constitution medicine is associated with polymorphisms of FCGR2A and *IL1RN* genes. *Neurol Res*. 2010;32(Suppl 1):43-47.

doi: 10.1179/016164109x12537002793922

74. Antequera-González B, Martínez-Micaelo N, Sureda-Barbosa C, *et al*. Specific multiomic profiling in aortic stenosis in bicuspid aortic valve disease. *Biomedicines*. 2024;12(2):380.

doi: 10.3390/biomedicines12020380

75. Gao Z, Fan S. The clinical and cellular impact of RBMS2 on the progression and prognosis of kidney renal clear cell carcinoma. *Genet Res (Camb)*. 2023;2023:5512781.

doi: 10.1155/2023/5512781

76. Liu L, McKeehan WL, Wang F, Xie R. MAP1S enhances autophagy to suppress tumorigenesis. *Autophagy*. 2012;8(2):278-280.

doi: 10.4161/auto.8.2.18939

77. He Y, Alejo S, Johnson JD, Jayamohan S, Sareddy GR. Reticulocalbin 3 is a novel mediator of glioblastoma progression. *Cancers (Basel)*. 2023;15(7):2008.

doi: 10.3390/cancers15072008

78. Poh AR, O'Donoghue RJ, Ernst M. Hematopoietic cell kinase (HCK) as a therapeutic target in immune and cancer cells. *Oncotarget*. 2015;6(18):15752-15771.

doi: 10.18632/oncotarget.4199

79. Qiao E, Huang Z, Wang W. Exploring potential genes and pathways related to calcific aortic valve disease. *Gene*. 2022;808:145987.

doi: 10.1016/j.gene.2021.145987

80. Bouchard D, Morisset D, Bourbonnais Y, Tremblay GM. Proteins with whey-acidic-protein motifs and cancer. *Lancet Oncol*. 2006;7(2):167-174.

doi: 10.1016/s1470-2045(06)70579-4

81. Majchrzak-Gorecka M, Majewski P, Grygier B, Murzyn K, Cichy J. Secretory leukocyte protease inhibitor (SLPI), a multifunctional protein in the host defense response. *Cytokine Growth Factor Rev*. 2016;28:79-93.

doi: 10.1016/j.cytogfr.2015.12.001

82. Zhu E, Shu X, Xu Z, *et al*. Screening of immune-related secretory proteins linking chronic kidney disease with calcific aortic valve disease based on comprehensive bioinformatics analysis and machine learning. *J Transl Med*. 2023;21(1):359.

doi: 10.1186/s12967-023-04171-x

Appendix

Table A1. Summary of the datasets used for IHS and CAVS research

Disease	Dataset	ID (Platform)	Cases	Controls	Type
IHS	GWAS	-	22,664	152,022	Exposure
CAVS	FinnGen	-	9,870	402,311	Outcome
IHS	GEO	GSE16561 (GPL6883)	39	24	Training set
IHS	GEO	GSE58294 (GPL570)	69	23	Validation set
CAVS	GEO	GSE83453 (GPL10558)	19	8	Training set
CAVS	GEO	GSE12644 (GPL570)	10	10	Validation set

Abbreviations: CAVS: Calcific aortic valve stenosis; GEO: Gene Expression Omnibus; GWAS: Genome-Wide Association Study; IHS: Ischemic stroke.

Table A2. Drug prediction results targeting the identified biomarkers

Symbol	Protein ID	Drug	Drug group	Pharmacological action
FCGR2A	P12318	Cetuximab	Approved	Unknown
		Etanercept	Approved, investigational	Unknown
		Human immunoglobulin G	Approved, investigational	Yes
		Abciximab	Approved	Unknown
		Alemtuzumab	Approved, investigational	Unknown
		Daclizumab	Investigational, withdrawn	Unknown
		Sarilumab	Approved, investigational	Unknown
		Catumaxomab	Approved, investigational, withdrawn	Yes
		Bevacizumab	Approved, investigational	Unknown
HCK	P08631	1-(ter-Butyl)-3-(p-tolyl)-1H-pyrazolo[3,4-d] pyrimidin-4-ylamine	Experimental	Unknown
		Phosphonotyrosine	Experimental	Unknown
		Quercetin	Experimental, investigational	Unknown
		Fostamatinib	Approved, investigational	Unknown
		Bosutinib	Approved	Yes
		Doramapimod	Investigational	Yes
		PP-121	Experimental	Yes

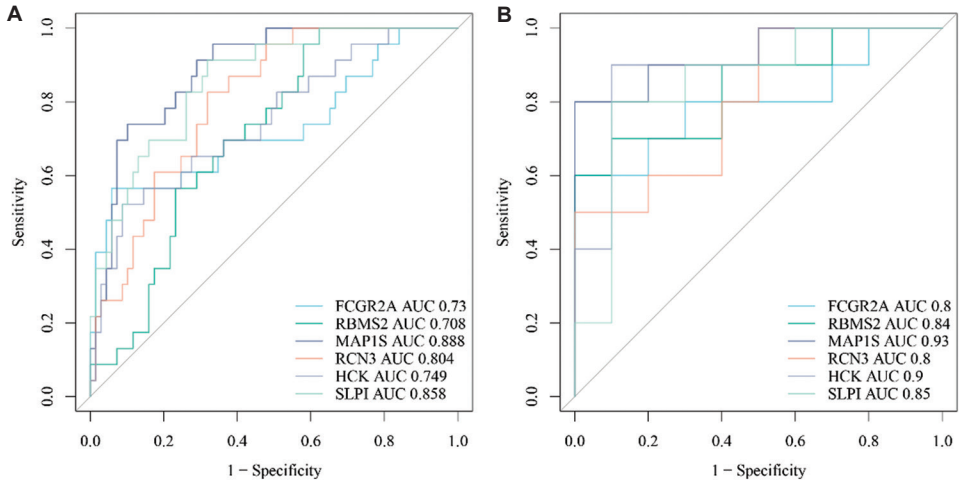

Figure A1. Validation of the diagnostic efficacy of candidate biomarkers in the validation set. (A) Receiver operating characteristic (ROC) curves of candidate biomarkers in the ischemic stroke set. (B) ROC curves of candidate biomarkers in the calcific aortic valve stenosis set. The area under the curve values for each biomarker are indicated in the legend

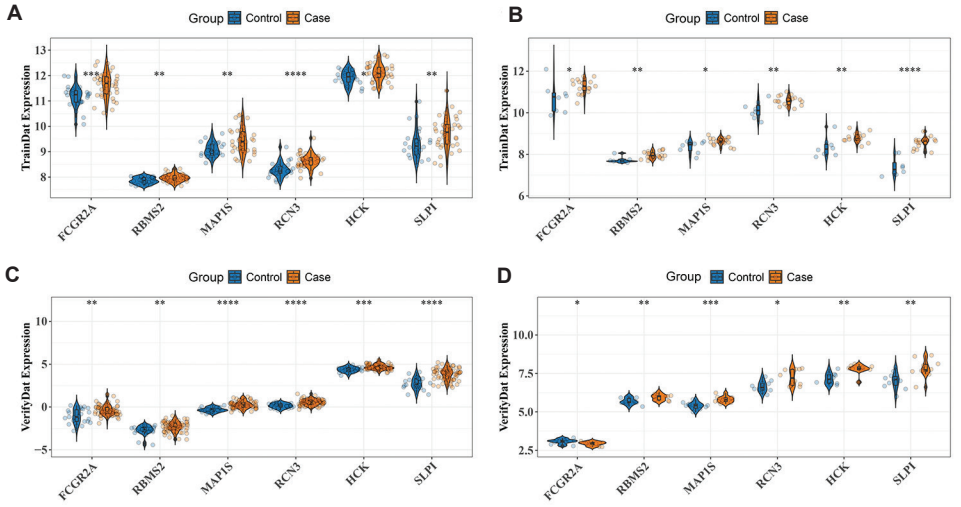

Figure A2. The expression patterns of the six biomarkers. (A) Expression patterns of six biomarkers in the ischemic stroke (his) training set. (B) Expression patterns of six biomarkers in the calcific aortic valve stenosis (CAVS) training set. (C) Expression patterns of six biomarkers in the IHS validation set. (D) Expression patterns of six biomarkers in the CAVS validation set. Blue represents the control group, and orange represents the disease group
Note: *$p \leq 0.05$; **$p \leq 0.01$; ***$p \leq 0.001$; ****$p \leq 0.0001$